Pergamon

Solid-State Electronics Vol. 42, No. 7–8, pp. 1481–1488, 1998

Printed in Great Britain

PII: S0038-1101(98)00054-9

0038-1101/98 $19.00 + 0.00

MICROSTRUCTURED THIN FILMS AND MULTILAYERS OF SUPERCONDUCTOR AND FERROMAGNETIC METAL

AKIKO ORITO, AKIKO FUKUSHIMA, SHINGO KATSUMOTO and YASUHIRO IYE

Institute for Solid State Physics, University of Tokyo, 7-22-1 Roppongi, Minato-ku, Tokyo 106, Japan

Abstract—We have investigated superconducting properties of thin films and multilayers consisting of superconductor/ferromagnet composite systems. Niobium thin films deposited on porous alumina exhibit a structure in the resistive transition curve near T_c at a field that is comparable to the matching field. A series of niobium/iron multilayers with different iron layer thicknesses show superconducting properties characteristic of decoupled layers. © 1998 Elsevier Science Ltd. All rights reserved

1. INTRODUCTION

A composite structure of superconductor and ferromagnet offers a unique opportunity for investigating and controlling the influence of magnetism on superconductivity. Much work has been focused on superconductor/ferromagnet multilayers with particular interest in the strong pair breaking effect and possible exotic superconducting states[1–5]. On the other hand, the recent development of microfabrication technique has made it possible to prepare microstructured superconductors, in which one can vary the relevant system size with respect to the various characteristic length scales of the problem[6]. Microstructured superconductor/ferromagnet composite systems provide a stage to investigate the interplay between superconductivity and magnetism on a microscopic scale[7].

In this paper we report our recent effort towards fabrication of microstructured mesoscopic superconductor/ferromagnet composite systems. Section 2 describes the fabrication of microstructured Nb films and Nb/Ni composite films using porous alumina as a substrate. Section 3 gives some preliminary results on the superconducting characteristics of Nb/Fe multilayers.

2. NB AND NB/NI COMPOSITE FILMS ON POROUS ALUMINA SUBSTRATE

2.1. *Sample preparation*

It is known that anode oxidation processing of high purity aluminum metal results in the formation of porous alumina with quasi-regular array of holes[8]. The radius of the holes can be controlled within a range of 0.01 to 1 μm by appropriate choice of oxidation conditions, such as the type and pH of the electrolytic solution and the bias voltage. In the present study, we have used such porous alumina membranes as substrate to produce nanostructured superconductor/ferromagnet systems.

The porous alumina membranes used in the present study are those commercially available as filter material (ANODISC, Whatman Co.). The structure of the porous alumina is schematically depicted in Fig. 1(a). Vertical holes of diameter 0.2 μm penetrate the 60 μm thick membrane. The in-plane distribution of the holes forms an approximate triangular lattice. The average distance between the neighboring holes is about 0.3 μm. The brims of the holes, therefore, form a quasi-regular honeycomb network. A scanning electron micrograph and atomic force micrograph reveal a high degree of surface roughness.

A 30 nm thick niobium film was sputter deposited on the surface of the porous alumina membrane. This resulted in a perforated film (or a quasi-honeycomb network) of Nb. On top of the Nb film, a 40 nm thick copper layer was deposited for the purpose of facilitating the subsequent electrochemical deposition process. The holes were partially filled with nickel by electrolytic deposition in a solution of $Ni(H_2NSO_3)_2{\cdot}4H_2O + NiCl_2{\cdot}6H_2O + H_2BO_3$. The nickel particles thus formed in the holes have a needle-like shape, 0.2 μm in diameter and a few μm in length. The length is proportional to the electrochemical deposition time and is only limited by the thickness of the membrane, 60 μm. Another sample was prepared in a similar way based on a 20 nm thick Nb film on a membrane with 0.02 μm diameter pores.

Magnetic properties of the Ni particles were characterized by measurements using a commercial SQUID magnetometer. The superconducting transition temperature and upper critical field of the Nb films with and without Ni particles were determined by standard low frequency ac resistivity measurements.

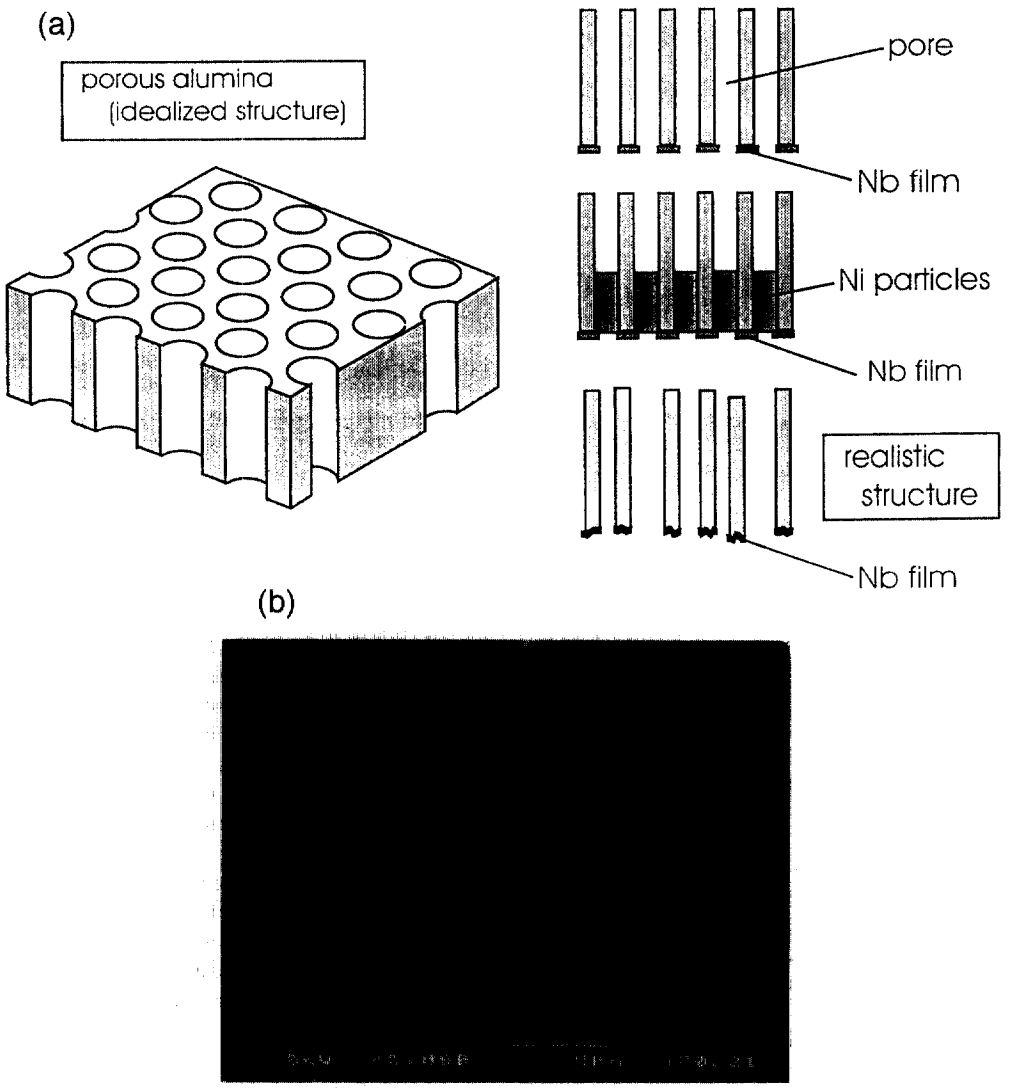

Fig. 1. (a) Schematic drawings of porous alumina and of Nb and Nb/Ni composite films. (b) Scanning electron micrograph showing a cross-sectional view of a porous alumina membrane of which the surface is covered by sputtered Nb thin film (white part on the left edge) and the pores are partially filled with electrochemically deposited nickel (densely packed white needles extending about 5 μm from the surface).

2.2. *Superconducting properties*

Figure 2 shows a series of resistive transition curves in a 30 nm thick Nb film on porous alumina under magnetic fields applied normal to the film plane at different temperatures. The superconducting critical field H_{c2} was defined by the midpoint of the resistive transition. Magnetoresistance curves similar to those in Fig. 2 taken for different field angles at a fixed temperature give the angular dependence of H_{c2} as shown in Fig. 3. In Figs 2 and 3, four sets of data are shown, i.e. Nb(30 nm) and Nb(20 nm) samples each with and without electrodeposited Ni particles.

The angular dependence of H_{c2} for the Nb(30 nm) films shown in Fig. 3 is somewhat unusual. In an ordinary thin film superconductor, the upper critical field shows such an anisotropy that H_{c2} is higher for a field parallel to the film plane. In a typical case, the angular dependence can be fitted to the Tinkham formula which has a characteristic cusp in $H_{c2}(\theta)$ at $\theta = 0$, i.e. field parallel to the plane[9] (see the data for Nb/Fe multilayers in Fig. 7). In the Nb(30) film by contrast, the anisotropy is relatively small and H_{c2} is larger for a field applied normal to the plane. The thinner film, Nb(20), shows an ordinary angular dependence of H_{c2}, but the anisotropy is far smaller than for a planar film of comparable thickness. The unusual behavior of the critical field anisotropy is presumably associated with the high degree of surface roughness in the brim of the pores.

Figure 4 shows the temperature dependence of H_{c2} for the two field orientations corresponding to

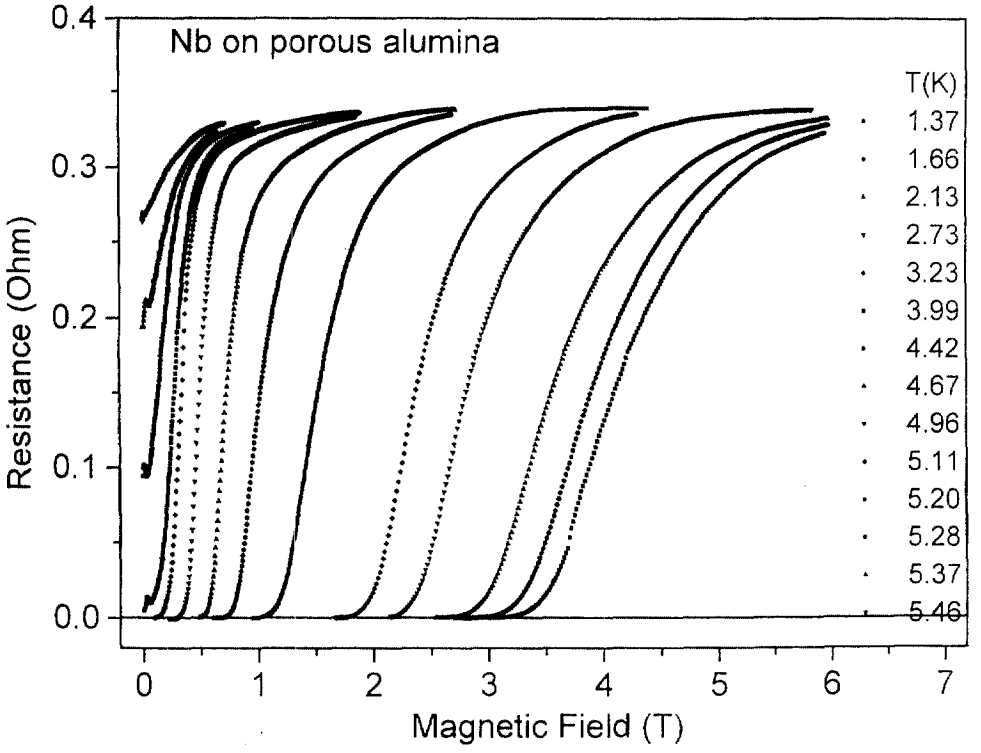

Fig. 2. Resistive transition curves as a function of magnetic field in a 30 nm thick Nb film deposited on a porous alumina substrate at different temperatures.

the H_{c2} maximum and minimum. The $H_{c2}(T)$ curve for the Nb(30) is linear in $1 - T/T_c$ for both field orientations. This behavior is again different from an ordinary thin film superconductor, in which case $H_{c2}(T)$ for the field parallel to the plane often exhibits a characteristic $(1 - T/T_c)^{1/2}$-dependence. The latter behavior is seen in the thinner film, Nb(20), near T_c.

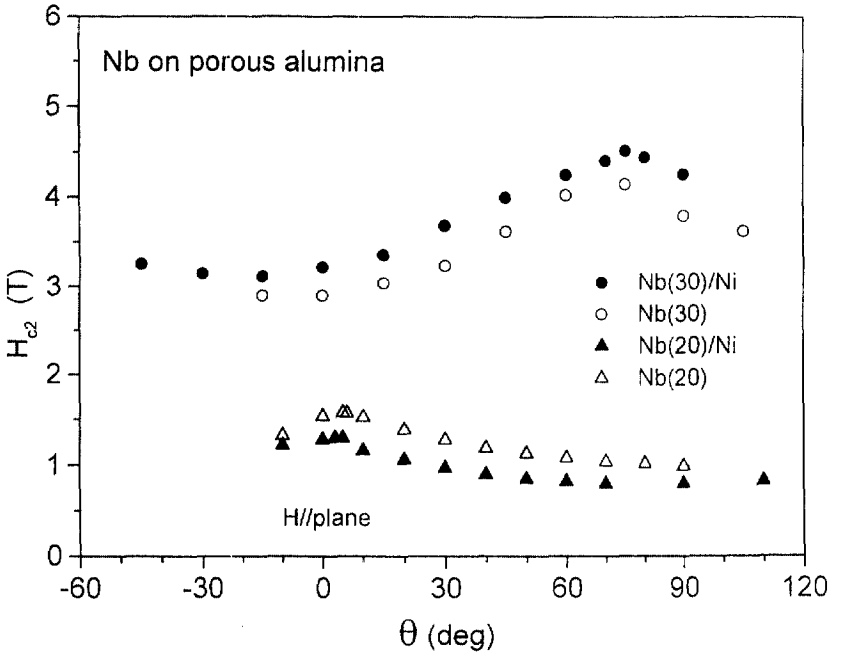

Fig. 3. Angular dependence of H_{c2} for four samples; 30 nm thick Nb films on an alumina substrate with 0.2 μm diameter pores and 20 nm thick ones on a substrate with 0.02 μm pores, each with and without electrochemically deposited Ni particles in the pores.

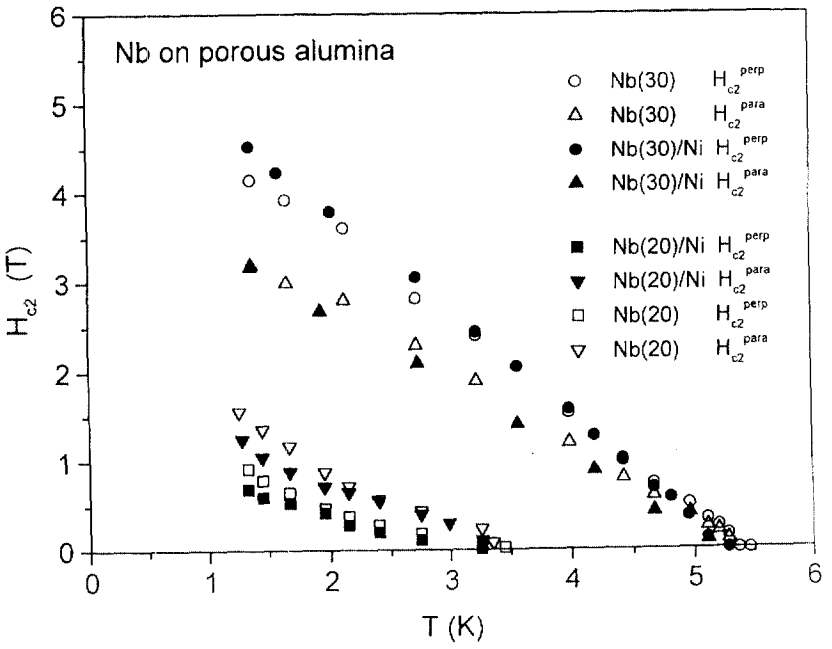

Fig. 4. Temperature dependence of the upper critical field for parallel and perpendicular field orientations for the four samples in Fig. 3.

In Fig. 2, a few traces taken at temperatures close to T_c show a small peak at low field. These are seen more clearly in the expanded plot of Fig. 5. The resistance peaks reside at about 20 mT and their position is found to be independent of temperature. This feature is attributed to commensurability of the flux lattice and the quasi-honeycomb network structure. The resistance minimum may reflect a maximum in $T_c(H)$ when the matching occurs. The value of the matching field, ~45 mT, translates to an average distance between the fluxoids of 0.21 μm. This value is very close to the average diameter, 0.2 μm, of the pores, but is smaller than the average distance between the pores, ~0.3 μm, as determined from the scanning electron micrograph. As the field is tilted away from the

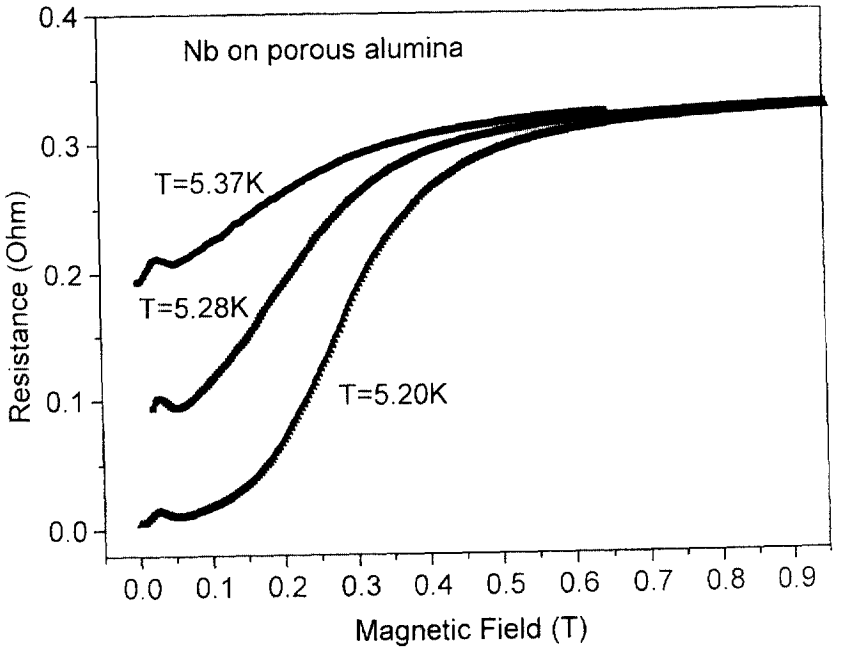

Fig. 5. The resistive transition curves in a Nb(30) film on porous alumina near T_c.

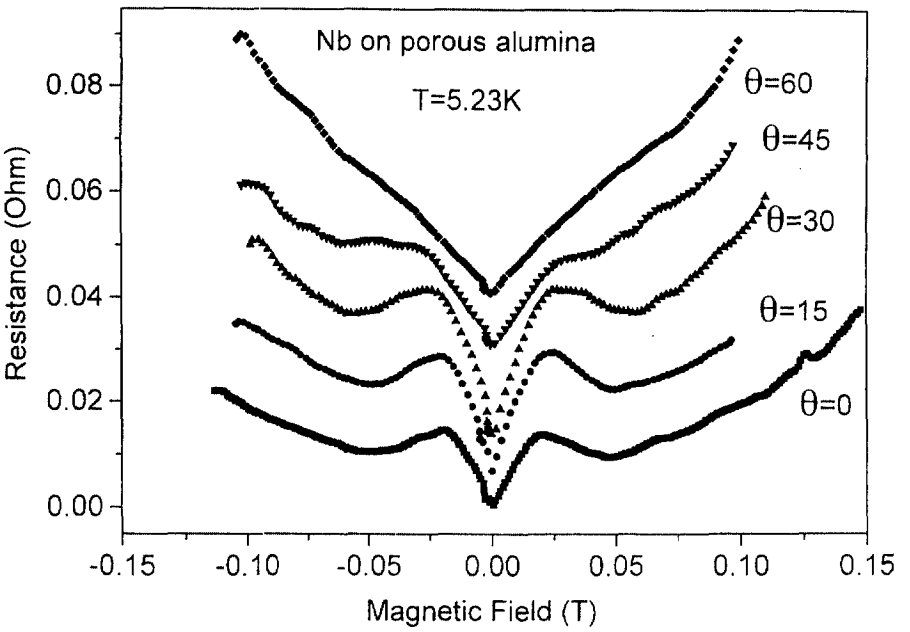

Fig. 6. Low field part of the resistive transition curves similar to those in Fig. 5 for different field orientations.

normal of the plane, the positions of the resistance maximum and minimum shift to higher fields as shown in Fig. 6. This is consistent with the above interpretation. At the same time, however, the feature is smeared at larger tilt angles. Such rapid smearing is presumably due to the surface roughness mentioned earlier, which effectively randomizes the area of individual loops projected to the field direction as the latter is tilted away from the surface normal.

Contrary to our expectation for significant influence of ferromagnetic Ni particle on the superconductivity of Nb, the sample with Ni particles did not show an outstanding difference from that without Ni, except for small suppression of T_c and a somewhat larger slope of $H_{c2}(T)$ for the perpendicular field. That the Ni particles are indeed ferromagnetic was confirmed by magnetization measurement. However, the average magnetic moment per Ni atom is apparently much smaller than the corresponding value for bulk metal. A possible reason for this is that part of the Ni atoms are in the form of hydroxide antiferromagnetic compounds such as nickel hydroxide. Another possible reason for the ineffectiveness of the Ni particles is that they are not in close contact with the Nb. The contact between the Ni particles in the holes and the Nb network on the brims may be quite small in area and an oxide layer may possibly lie in between. If such is the case, the pair breaking effect will be greatly suppressed and the only effect of the Ni particles will be relatively minor modification of the local field.

3. Nb/Fe MULTILAYERS

3.1. *Sample preparation*

Multilayer samples of Nb/Fe were prepared on SiO_2/Si(100) substrates by an rf-sputtering technique. The sputtering system is equipped with three sputter guns and a stepping-motor-controlled shutter. The base pressure of the chamber was 3×10^{-8} torr. Prior to the deposition the evaporation rate from each sputter gun was calibrated by quartz oscillator thickness monitor. Multilayer samples were prepared by alternating deposition of constituent metals by appropriate sequencing of the shutter control. Typically 10 units were deposited. In the present study, the thickness of the Nb layer was fixed at 30 nm and that of the Fe layer was varied. Several samples with different Fe layer thicknesses were prepared individually. We also tried another approach by making a long sample with the Fe layer thickness continuously varied from one end to the other. This was achieved by sweeping a second shutter in front of the substrate during the deposition of Fe.

3.2. *Superconducting properties*

The anisotropy and temperature dependence of the upper critical field were investigated for a series of Nb/Fe multilayers with different Fe layer thicknesses. Figure 7 shows the angular dependence of H_{c2} for a few Nb/Fe multilayer samples. Data for a single layer of Nb and a Nb/Cu multilayer sample are also shown for comparison. All these curves exhibit a cusp at $\theta = 0$ characteristic of well-

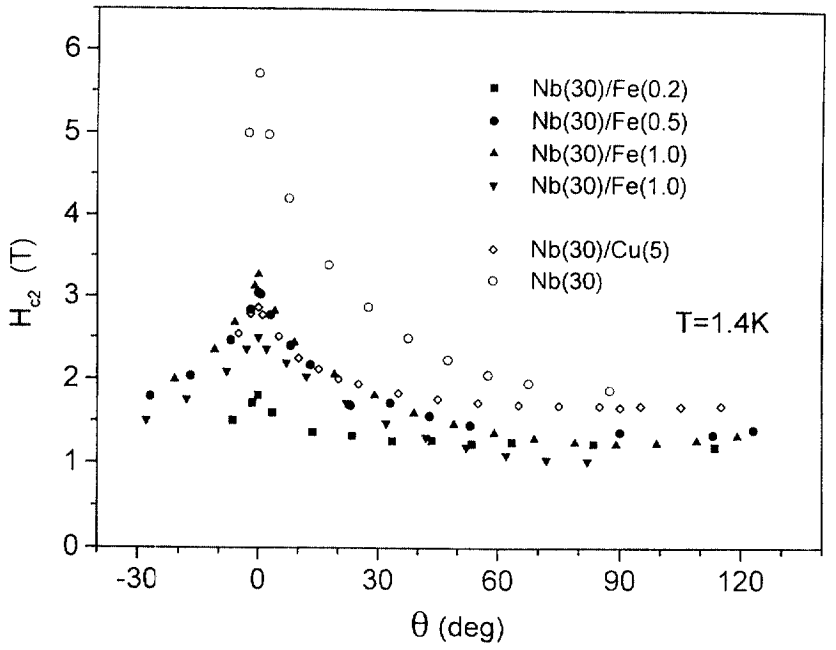

Fig. 7. Angular dependence of H_{c2} in a series of Nb/Fe multilayers at $T = 1.4$ K. Data for a Nb/Cu multilayer and a Nb single layer are also shown.

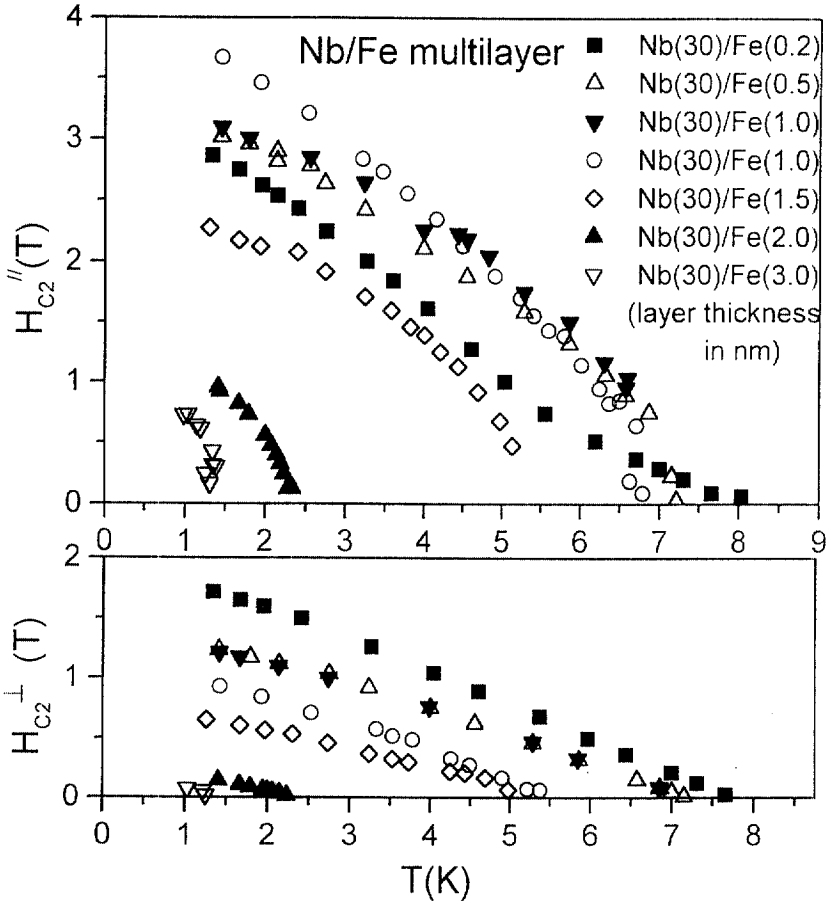

Fig. 8. Temperature dependence of H_{c2} in a series of Nb/Fe multilayers for parallel and perpendicular field orientations.

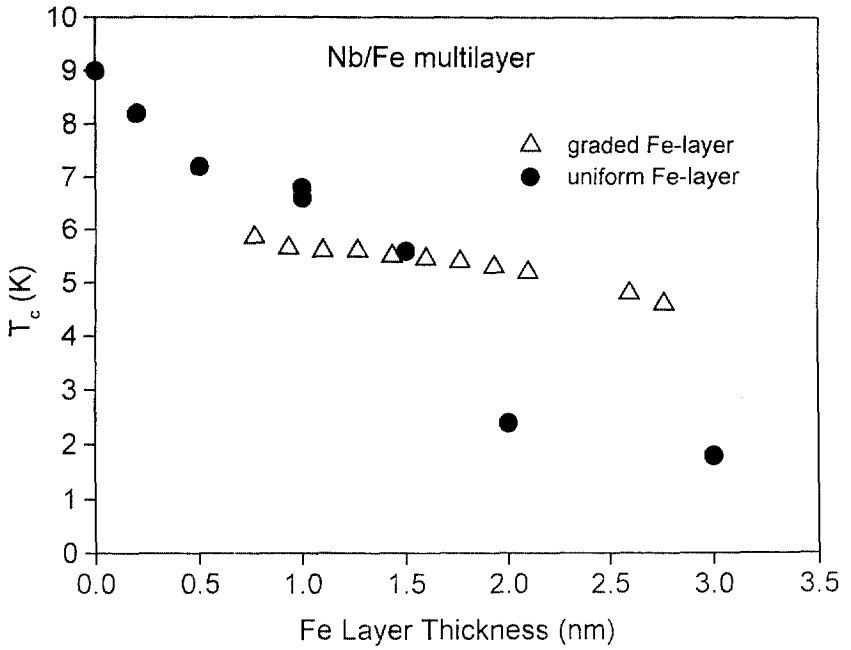

Fig. 9. The dependence of T_c on the Fe layer thickness for Nb/Fe multilayers with fixed Nb layer thickness 30 nm. The circles are the data for the individually prepared samples, while the triangles represent a set of data taken for the sample with graded Fe layer thickness.

decoupled superconducting layers. As expected, the ferromagnetic Fe layer is much more effective than the nonmagnetic Cu layer in decoupling the interlayer coherence, as evidenced by the larger anisotropy in the Fe 0.5 nm multilayer than in the Cu 5 nm multilayer.

Figure 8 shows $H_{c2}(T)$ for field orientations parallel and perpendicular to the layer. With the field applied parallel to the layer, $H_{c2}(T)$ shows a $(1 - T/T_c)^{1/2}$-dependence characteristic of the 2D nature of superconductivity. In the case of the Nb(30)/Fe(0.2) multilayer, the parallel critical field clearly shows dimensional crossover behavior, i.e. $H_{c2}(T)$ is linear in $(1 - T/T_c)$ near T_c but switches to the 2D like $(1 - T/T_c)^{1/2}$-dependence at lower temperatures.

Figure 9 summarizes the dependence of T_c on the thickness of the Fe layer for a series of Nb/Fe multilayers with the Nb layer thickness fixed at 30 nm. The solid circles are individually prepared samples and the open triangles represent a set of data taken for a sample with graded Fe layer thickness. The origin of the discrepancy between the two sets of data at larger Fe layer thickness is not understood at the moment. The behavior of T_c in superconductor/ferromagnet multilayer systems have been studied by several groups. A non-monotonic or oscillatory dependence of T_c on the ferromagnetic layer thickness is reported for Nb/Gd multilayers[5] which is taken to be caused by an intrinsic phase difference by π at the superconductor/ferromagnet interface[10]. On the other hand, the absence of such an oscillatory dependence is reported for V/Fe multilayers[3]. The present data for the Nb/Fe system although still preliminary seem to indicate a monotonic change of T_c with Fe layer thickness. To decide whether a similar effect may be present in the Nb/Fe system, it is necessary to accumulate systematic data. The use of graded Fe layer samples is advantageous in minimizing fluctuations in the thickness and quality of the Nb layer to which T_c is sensitive.

4. CONCLUSIONS

In this paper we reported our effort to explore physics in superconductor/ferromagnet composite systems. The electrochemical deposition of metals into the holes of porous alumina is a unique method to fabricate a quasi-regular array of elongated particles. The Nb/Fe multilayer system exhibits characteristics of well-decoupled superconducting layers. In the study of superconductor/ferromagnet composite systems, it is advantageous to combine appropriately the microfabrication techniques and multilayer growth, because some of the relevant length scales (e.g. Cooper pair penetration into the ferromagnet) are generally smaller than those controllable by the standard microfabrication techniques.

Acknowledgements—The authors are grateful to Professor H. Masuda of Tokyo Metropolitan University for providing helpful information on anodic porous alumina and to Mr M. Isobe and Professor Y. Ueda of ISSP for help with SQUID magnetization measurements.

REFERENCES

1. Jin, B. Y. and Ketterson, J. B., *Adv. Phys.*, 1989, **38,** 189 (and references therein).
2. Wong, H. K., Jin, B. Y., Yang, H. Q., Ketterson, J. B. and Hilliard, J. E., *J. Low Temp. Phys.*, 1986, **63,** 307.
3. Koorevaar, P., Suzuki, Y., Coehoorn, R. and Aarts, J., *Phys. Rev. B*, 1994, **49,** 441.
4. Strunk, C., Suerger, C., Paschen, U. and v. Loehneysen, H., *Phys. Rev. B*, 1994, **49,** 4053.
5. Jiang, J. S., Davidovic, D., Reich, D. H. and Chien, C. L., *Phys. Rev. Lett.*, 1995, **74,** 314.
6. Lykov, A. N., *Adv. Phys.*, 1993, **42,** 263 (and references therein).
7. Otani, Y., Pannetier, B., Nozires, J. P. and Givord, D., *J. Mag. Mag. Mater.*, 1993, **126,** 622.
8. Masuda, H. and Fukuda, K., *Science*, 1995, **268,** 1466 (and references therein).
9. Tinkham, M., *Introduction to Superconductivity*, 2nd edn. McGraw-Hill, New York, 1996.
10. Bulaevskii, L. N., Kuzii, V. V. and Sobyanin, A. A., *Pis'ma Zh. Eksp. Teor. Fiz.*, 1977, **25**, 314 (*JETP Lett.*, 1977, **25**, 290).